

# A distortion of very-high-redshift galaxy number counts by gravitational lensing

J. Stuart B. Wyithe<sup>1</sup>, Haojing Yan<sup>2</sup>, Rogier A. Windhorst<sup>3</sup> & Shude Mao<sup>4,5</sup>

The observed number counts of high-redshift galaxy candidates<sup>1–8</sup> have been used to build up a statistical description of star-forming activity at redshift  $z \gtrsim 7$ , when galaxies reionized the Universe<sup>1,2,9,10</sup>. Standard models<sup>11</sup> predict that a high incidence of gravitational lensing will probably distort measurements of flux and number of these earliest galaxies. The raw probability of this happening has been estimated to be  $\sim 0.5$  per cent (refs 11, 12), but can be larger owing to observational biases. Here we report that gravitational lensing is likely to dominate the observed properties of galaxies with redshifts of  $z \gtrsim 12$ , when the instrumental limiting magnitude is expected to be brighter than the characteristic magnitude of the galaxy sample. The number counts could be modified by an order of magnitude, with most galaxies being part of multiply imaged systems, located less than 1 arcsec from brighter foreground galaxies at  $z \approx 2$ . This lens-induced association of high-redshift and foreground galaxies has perhaps already been observed among a sample of galaxy candidates identified at  $z \approx 10.6$ . Future surveys will need to be designed to account for a significant gravitational lensing bias in high-redshift galaxy samples.

Along random lines of sight, the raw probability (or optical depth) of multiple imaging of objects at high redshifts—owing to gravitational lensing by individual foreground field galaxies<sup>11,12</sup>—is  $\sim 0.5\%$ . However, all galaxy populations are observed to have a characteristic luminosity ( $L_*$ ), brighter than which galaxy numbers drop exponentially, and below which numbers rise with a very steep power-law slope<sup>14,6</sup>. The potential for gravitational lensing to modify the observed statistics therefore increases dramatically, owing to the magnification of numerous, intrinsically faint galaxies to observed fluxes that are above the survey limit. This effect, which is known as magnification bias<sup>13</sup>, leads to an excess of gravitationally lensed galaxies among flux-limited samples. Magnification bias is expected to be particularly significant at high redshifts ( $z \gtrsim 8$ ), where current observations may only be probing the exponential tail of the luminosity function<sup>4</sup>, so that the number density could be rising very rapidly towards the detection limit. Indeed, multiply imaged candidates at  $z \gtrsim 7$  have already been discovered behind foreground clusters via targeted searches<sup>14–16</sup>, demonstrating this to be an efficient method for finding faint high-redshift galaxies<sup>14,17</sup>.

We assess magnification bias among high-redshift galaxies assuming singular, spherical, isothermal gravitational lenses, which produce one or two images, and designate the apparent magnitude of the more magnified image (the only image in the absence of lensing) as  $m_{AB,1}$ . We then calculate, as a function of the assumed characteristic luminosity (expressed in terms of absolute magnitude,  $M_*$ ), the fraction of galaxies brighter than the magnitude limit ( $m_{lim}$ ) for the Hubble Ultra Deep Field (HUDF) that would be multiply imaged (designated  $F_{lens}$ ). Such curves are shown at  $z = 6, 7, 8.6$  and  $10.6$  in Fig. 1a. The superimposed filled and open points correspond to lens fractions for different estimates<sup>14</sup> of  $M_*$  at these redshifts. At  $z \approx 6–7$ , we expect only  $\sim 1\%$  of galaxies to be lensed. At  $z \approx 8–10$ , however, we expect a lensed fraction

of a few to a few tens of per cent, depending on the true value of  $M_*$ . Note that since current survey limits are significantly fainter than  $M_*$  at  $z \approx 6–7$ , the lens fraction is quite insensitive to  $M_*$ . However, at higher redshifts where the survey limits might be much closer to  $M_*$ , the lensing fraction is very sensitive to its uncertain value.

Predictions for a significant lens fraction at  $z \gtrsim 8$  stand in apparent contrast to the fact that no image pairs have been identified in the HUDF. However, we find the probability that a multiply imaged galaxy, with observed  $m_{AB,1}$  has a corresponding second image with  $m_{AB,2} < m_{lim}$  (that is, detectable with the HUDF data) to be only  $\sim 10\%$ , even for galaxies that are one magnitude brighter than  $m_{lim}$  (Supplementary Information). Thus, as shown in Fig. 1b, the fraction of galaxies ( $F_{mult}$ ) that are detected as multiply imaged systems in the HUDF is an order of magnitude lower than the true lensed fraction. Although this fraction would increase somewhat if elliptical lenses were included in our analysis, multiply imaged systems are not expected to be observed in the current data. On the other hand, magnification bias also leads to a concentration of high-redshift sources—both singly and multiply imaged—around foreground galaxies<sup>18–20</sup>. The resulting correlation between high-redshift candidates and bright foreground galaxies therefore offers an alternative avenue to observing the effect of gravitational lensing. A schematic diagram illustrating this point, as well as magnification bias, is included as Supplementary Fig. 1.

To quantify this correlation, we first determine the distribution of separations between random lines of sight and the nearest bright ( $H \leq 25$  mag) foreground galaxy in the HUDF, measured as the angular distance to the centroid. This is shown by the dotted black line in Fig. 1c. This distribution can be compared to the predictions of our model (black dashed line in Fig. 1c). If the candidate sample consists of both multiply imaged and unmagnified galaxies, then the observed distribution of separations should be a weighted sum of the random and the lensed line-of-sight distributions. The correct weighting is the probability for gravitational lensing,  $F_{lens}$ . Two examples (blue dotted and dashed lines) are shown in Fig. 1c. The fraction of galaxies found within  $\Delta\theta \approx 1–2$  arcsec of a foreground galaxy is very sensitive to the characteristic luminosity if  $M_* \gtrsim -19$  mag, providing a potential observable for the influence of lensing on the number counts of  $z \gtrsim 8$  candidates.

For comparison with the lensing predictions, we have measured the distribution of separations between a sample of  $z \approx 10.6$  candidates<sup>4</sup> and their nearest bright ( $H \leq 25$  mag) foreground galaxy. Comparing the distributions, we find that these candidates are observed to be closer to bright foreground galaxies than are random lines of sight. On the other hand, the candidates are found at larger separations from foreground galaxies than would be predicted if they were all multiply imaged. Quantitatively, the Kolmogorov–Smirnov probabilities between the observed distributions and the all-random model or the all-lensed model (Supplementary Information) indicate that both models are rejected at high significance. This suggests that a fraction of candidates may be gravitationally lensed. Moreover, we have generated the

<sup>1</sup>School of Physics, University of Melbourne, Parkville, Victoria 3010, Australia. <sup>2</sup>Center for Cosmology and AstroParticle Physics, The Ohio State University, Columbus, Ohio 43210, USA. <sup>3</sup>School of Earth and Space Exploration, Arizona State University, Tempe, Arizona 85287-1404, USA. <sup>4</sup>Jodrell Bank Centre for Astrophysics, University of Manchester, Manchester M13 9PL, UK. <sup>5</sup>National Astronomical Observatories of China, Chinese Academy of Sciences, Beijing 100012, China.

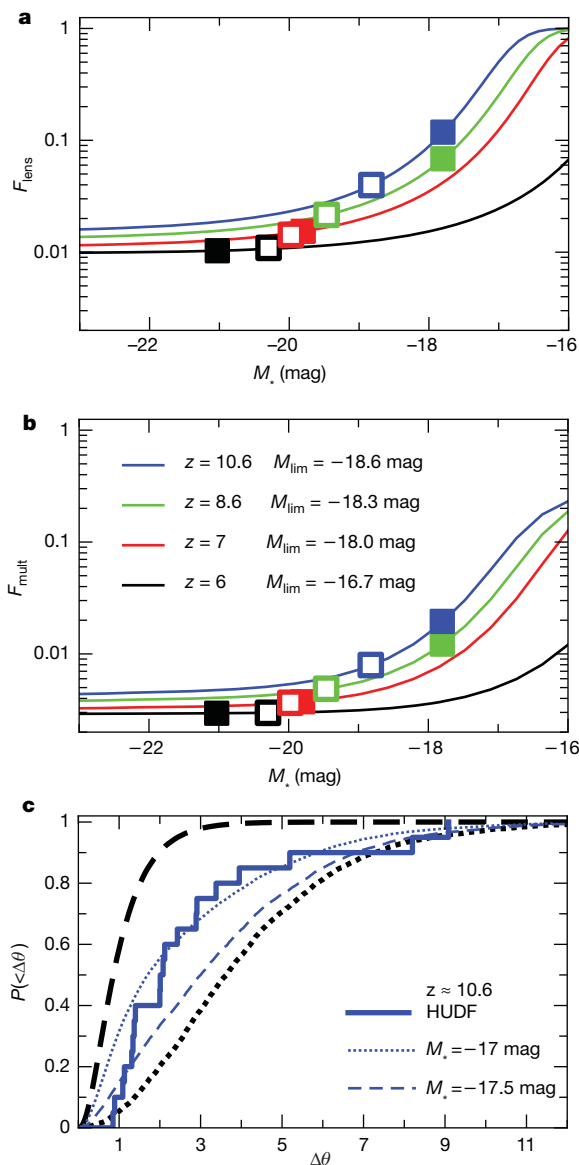


**Figure 1 | Gravitational lens fractions among candidate high-redshift HUDF galaxies.** **a**, The fraction of multiply imaged high-redshift galaxies (with  $m_{AB,1} < m_{lim}$ ). **b**, The fraction of high-redshift galaxies in which multiple images could be detected in the HUDF (with  $m_{AB,2} < m_{lim}$ ). **c**, The probability distribution of image separations (at  $z \approx 10.6$ ) relative to the nearest bright foreground galaxy, in the cases of random lines-of-sight (black dotted line), of gravitational lenses (black dashed line), and for composite distributions computed for two (faint) values of  $M_*$  (blue dotted and dashed lines). Also shown is the distribution of measured separations for 20  $z \approx 10.6$  candidates<sup>4</sup> in the HUDF (stepped blue histogram). Results in **a**, **b** and **c** correspond to samples of Lyman-break galaxy candidates selected with median redshifts of  $z \approx 6$ ,  $z \approx 7$ ,  $z \approx 8.6$  and  $z \approx 10.6$ . At  $z \approx 6$ , candidate selection using the Advanced Camera for Surveys reaches<sup>6</sup>  $m_{lim} = 30$  mag (absolute magnitude  $M_{lim} = -16.7$  mag). At higher redshifts, objects in the WFC3 HUDF data can be selected<sup>4</sup> to  $m_{lim} \approx 29.0$  mag, corresponding to  $M_{lim} = -18.0$ ,  $-18.3$  and  $-18.6$  mag at  $z \approx 7$ ,  $8.6$  and  $10.6$ . In **a** and **b** the open squares correspond to lens fractions given the fitting formula<sup>1,25</sup>  $M_* \approx -21 + 0.32 \times (z - 3.8)$ , and the filled squares represent alternative estimates<sup>4,6</sup> of  $M_*$ . The model for gravitational lensing<sup>26</sup> is based on the velocity dispersion function of galaxies<sup>27</sup>. Galaxy mass distributions are modelled as singular isothermal spheres, and we assume a constant co-moving density of lenses. Elliptical lenses would not significantly alter the cross-section<sup>28</sup>, but would provide additional images, and so increase the fraction of observed galaxies that are lensed. We assume a Schechter luminosity function<sup>22</sup>, with power-law slope<sup>1</sup>  $\alpha = -2$ . A change of 0.3 in  $\alpha$  leads to a 40% change in the lens probability. We have used the cosmology based on 7-year results from the WMAP satellite<sup>29</sup> throughout this Letter.

distribution of redshifts for foreground galaxies found within  $\Delta\theta < 1.5$  arcsec of the  $z \approx 10.6$  candidates. These distributions are consistent with the distribution of gravitational lens redshifts, while the redshift distribution of all bright foreground galaxies are not, which supports the hypothesis that foreground galaxies are lensing a fraction of the  $z \approx 10.6$  candidates into the observed sample.

With the introduction of the James Webb Space Telescope (JWST), galaxy surveys will be undertaken out to even higher redshifts, well into the epoch of first light<sup>21</sup>. We show  $F_{lens}$  as a function of  $M_*$  out to  $z = 20$  in Fig. 2a, b. The flux limits correspond to an ultra-deep survey ( $m_{lim} = 31.4$  mag), and a medium-deep survey ( $m_{lim} = 29.4$  mag). The evolution of the characteristic luminosity is unknown at these unexplored redshifts. For comparison, we therefore plot squares corresponding to estimates of  $M_*$  based on an extrapolation from lower redshift HUDF data<sup>1</sup>. Figure 2 shows that in ultra-deep JWST surveys for first light objects at  $z \gtrsim 14$ , more than  $F_{lens} \approx 10\%$  of the candidates could be lensed. In much shallower JWST surveys that only sample the **exponential tail of the Schechter luminosity function**, a lensed object fraction of  $F_{lens} \approx 10\%$  could be seen at redshifts as low as  $z \approx 8-10$ . However at  $z \gtrsim 14$ , the lensed fraction in such surveys could be much higher, and may even represent the majority of observed galaxies. Surveys with JWST will therefore need to be carefully planned and analysed to account for the influence of foreground lensing galaxies.

As in the case of the HUDF, the fraction of galaxies that will be detected as multiply imaged systems by JWST is significantly lower than the true multiple image fraction. However, as the multiple image fraction becomes very large at high redshifts, observed doubles could become common; larger than  $F_{mult} \approx 10\%$  at redshifts  $z \gtrsim 12$  in a medium-deep ( $m_{AB} < 29.4$  mag) JWST survey, and  $z \gtrsim 16$  in an ultra-deep ( $m_{AB} < 31.4$  mag) survey. In Fig. 2e, f, we present the predicted distributions of separation for galaxies discovered by JWST from bright foreground galaxies. If the observed evolution in  $M_*$  continues to higher redshift, then the spatial distribution of high-redshift galaxies relative to foreground galaxies will depart from random at redshifts  $z \gtrsim 14$  for ultra-deep surveys, and at  $z \gtrsim 10$  for medium-deep surveys with JWST. A crucial prediction is that the majority of very-high-redshift galaxies discovered with JWST may be located less than 1 arcsec from a bright foreground galaxy, and will have been gravitationally magnified into the sample.

A key goal for JWST will be to measure the number counts of high-redshift candidates, and to construct luminosity functions in order to build up a statistical description of star-forming activity in galaxies. Luminosity functions describing the density of sources per unit luminosity are parametrized by a Schechter function<sup>22</sup>,  $\Psi(L) \propto (L/L_*)^\alpha \exp(-L/L_*)$ , including free parameters for the power-law slope at low luminosities ( $\alpha$ ), and the characteristic absolute AB-magnitude ( $M_{AB} - M_* = -2.5 \log_{10}(L/L_*)$ ) brighter than which galaxy numbers drop exponentially. Importantly, gravitational lensing has the potential to significantly modify the observed luminosity function from its intrinsic shape<sup>23</sup>. In particular, at very high luminosities in the exponential tail of the Schechter function, the shape can be modified from exponential to power-law, since gravitational lensing magnifies numerous faint sources to apparently higher luminosities. Figure 3 shows that the shapes of luminosity functions near the flux limit are not affected by gravitational lensing at  $z \approx 6-8$ . However, if the evolution of the galaxy luminosity function continues into the reionization era (we assume an extrapolation of the fitting formulae based on candidates discovered in and around the HUDF<sup>1</sup>), then we find that JWST will measure luminosity functions that are significantly modified by lensing at redshifts above  $z \approx 14$  and  $z \approx 10$  in its ultra-deep and medium-deep surveys, respectively.

Our results imply that although published luminosity functions at  $z \gtrsim 7$  are not currently corrected for a potential gravitational lensing bias, such corrections will need to be prescribed in detail for future surveys using JWST that aim to measure the build-up of stellar mass among the first galaxies. In particular, studies of the high-redshift

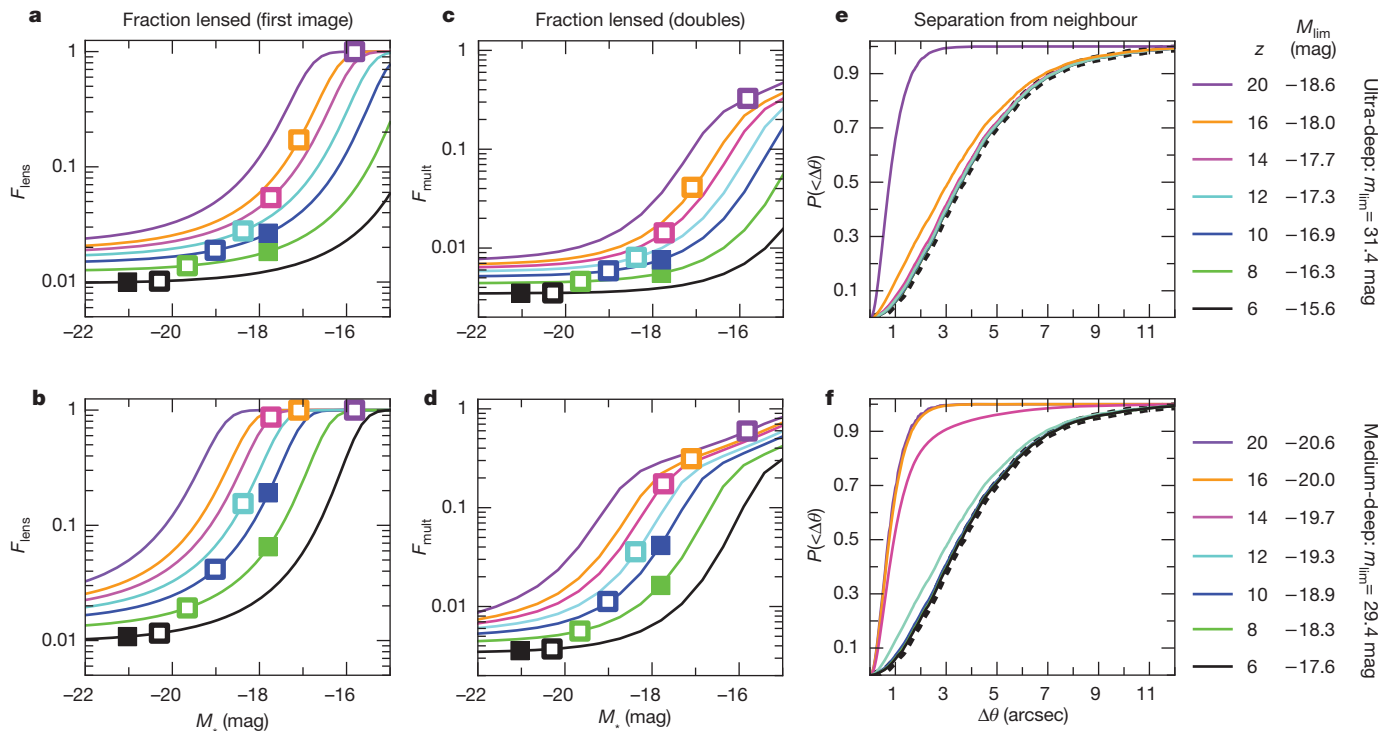


**Figure 2 | Probabilities of multiple imaging of high-redshift galaxies with JWST.** The panels mirror those of Fig. 1, but with examples of limiting magnitudes and redshifts appropriate for both an ultra-deep survey (top row:  $m_{\text{lim}} = 31.4$  mag,  $\sim 1$  nJy), and a medium-deep survey (bottom row:  $m_{\text{lim}} = 29.4$  mag) with JWST. The corresponding limiting absolute magnitudes are listed at right. **a, b,** The fraction of observed galaxies that have multiple images (with  $m_{\text{AB},1} < m_{\text{lim}}$ ). The superimposed filled and open points correspond to lens fractions given a faint value<sup>4</sup> of  $M_* = -17.8$  at  $z \approx 8.6$  and  $z \approx 10.6$ , and a fitting formula  $M_*(z)$  based on lower redshift data, respectively<sup>1,25</sup>. The latter is extrapolated to high redshift where data does not yet exist. **c, d,** The fraction of high-redshift galaxies in which multiple images

could be detected by JWST (with  $m_{\text{AB},2} < m_{\text{lim}}$ ). **e, f,** The probability distribution of image separations relative to the nearest bright foreground galaxy, in the cases of random lines of sight (black dotted line), and for composite distributions computed for values of  $M_*$  extrapolated from observations in the HUDF using the previously mentioned fitting formula<sup>1,25</sup>. We note that imaging surveys with JWST will be working at the diffraction limit ( $\sim 0.08$  arcsec resolution FWHM) at  $\sim 2 \mu\text{m}$ . This resolution is higher than is currently available in the HUDF near-infrared images, where candidates have been selected in close proximity to bright foreground galaxies, and hence high-redshift candidates will also be detectable close to foreground galaxies.

luminosity function will require good understanding of the magnification bias for high-redshift galaxies, in order to correct for gravitational lensing and uncover its true unlensed shape at  $z \gtrsim 12$ . Of particular importance will be the unknown evolution of  $M_*$ , which could be influenced (for example) by supernova feedback from population-III stars<sup>24</sup>, in addition to hierarchical clustering and formation. Gravitational lensing could magnify objects at  $z \gtrsim 10$ – $12$  to flux levels that will allow spectroscopic observations using JWST and the largest ground-based near-infrared spectrographs. A further implication of our analysis is that gravitational lensing could be used to probe the shape of the high-redshift luminosity function at luminosities that are not otherwise accessible<sup>12</sup>, using the association of high-redshift galaxy

candidates and foreground galaxies, combined with careful modelling of the gravitational lensing bias.

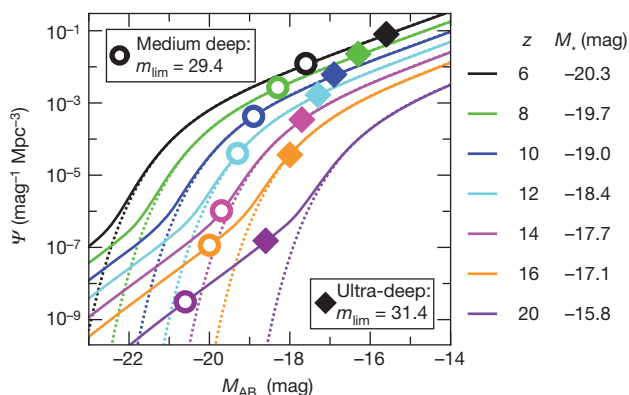


**Figure 3 | Gravitational-lens-induced modification of the bright end of the high-redshift galaxy luminosity function to be observed with JWST.** Dotted curves present the intrinsic luminosity function ( $\psi$ ), and solid curves the observed luminosity function following modification from gravitational lensing. For simplicity, a uniform magnification was assumed outside regions of sky that are multiply imaged, with a value such that flux is conserved over the whole sky. The parameters describing the luminosity function are extrapolated to high redshift, where data do not yet exist, assuming fitting formulae based on data from the HUDF<sup>1,25</sup>. Of particular relevance are the values of  $M_*$ , which are listed (right). The filled and open points show the luminosities and densities of the faintest galaxies to be observed with JWST, assuming limiting magnitudes appropriate for both an ultra-deep JWST survey ( $m_{\text{AB}} < 31.4$  mag), and a medium-deep JWST survey ( $m_{\text{AB}} < 29.4$  mag). The probability of gravitational lensing will become of order unity in the steep exponential parts of the luminosity function at sufficiently high redshifts. This gravitational forest should not be confused with the purely mathematical effects of image crowding that makes the detection and de-blending of faint objects harder at progressively fainter fluxes<sup>30</sup>. These latter effects are referred to as either the instrumental confusion limit—when the instrumental resolution is not good enough to statistically distinguish all faint background objects from brighter foreground objects—or the natural confusion limit—when the instrumental resolution is good enough to distinguish faint background objects from brighter foreground objects, but the images are so deep that objects start overlapping because of their own intrinsic sizes. The HUDF and JWST images are in the latter regime<sup>30</sup>, and as argued in this Letter, probably have the additional fundamental limitation that gravitational lensing will magnify a non-negligible fraction of faint objects into the sample.



Received 21 July; accepted 27 October 2010.

1. Bouwens, R. J. *et al.* UV luminosity functions from 113  $z \sim 7$  and  $z \sim 8$  Lyman-break galaxies in the ultra-deep HUDF09 and wide-area ERS WFC3/IR observations. Preprint at (<http://arxiv.org/abs/1006.4360>) (2010).
2. Lorenzoni, S. *et al.* Candidate  $z \sim 8-9$  galaxies from WFC3 imaging. Preprint at (<http://arxiv.org/abs/1006.3545>) (2010).
3. Bouwens, R. J. *et al.* Constraints on the first galaxies:  $z \sim 10$  galaxy candidates from HST WFC3/IR. Preprint at (<http://arxiv.org/abs/0912.4263>) (2009).
4. Yan, H. *et al.* Galaxy formation in the reionization epoch as hinted by Wide Field Camera 3 observations of the Hubble Ultra Deep Field. *Res. Astron. Astrophys.* **10**, 867–904 (2010).
5. Bouwens, R. J. *et al.* Star formation at  $z \sim 6$ : the Hubble Ultra Deep Parallel Fields. *Astrophys. J.* **606**, L25–L28 (2004).
6. Yan, H. & Windhorst, R. A. Candidates of  $z \sim 5.5-7$  galaxies in the Hubble Space Telescope Ultra Deep Field. *Astrophys. J.* **612**, L93–L96 (2004).
7. Wilkins, S. M. *et al.* Probing  $L^*$  Lyman-break galaxies at  $z \sim 7$  in GOODS-South with WFC3 on Hubble Space Telescope. *Mon. Not. R. Astron. Soc.* **403**, 938–944 (2010).
8. McLure, R. J. *et al.* Galaxies at  $z = 6-9$  from the WFC3/IR imaging of the Hubble Ultra Deep Field. *Mon. Not. R. Astron. Soc.* **403**, 960–983 (2010).
9. Yan, H. & Windhorst, R. A. The major sources of the cosmic reionizing background at  $z \sim 6$ . *Astrophys. J.* **600**, L1–L5 (2004).
10. Trenti, M. *et al.* The galaxy luminosity function during the reionization epoch. *Astrophys. J.* **714**, L202–L207 (2010).
11. Barkana, R. & Loeb, A. High-redshift galaxies: their predicted size and surface brightness distributions and their gravitational lensing probability. *Astrophys. J.* **531**, 613–623 (2000).
12. Comerford, J. M., Haiman, Z. & Schaye, J. Constraining the redshift  $z \sim 6$  quasar luminosity function using gravitational lensing. *Astrophys. J.* **580**, 63–72 (2002).
13. Turner, E. L., Ostriker, J. P. & Gott, J. R. III. The statistics of gravitational lenses—the distributions of image angular separations and lens redshifts. *Astrophys. J.* **284**, 1–22 (1984).
14. Richard, J. *et al.* A Hubble and Spitzer Space Telescope survey for gravitationally lensed galaxies: further evidence for a significant population of low-luminosity galaxies beyond  $z = 7$ . *Astrophys. J.* **685**, 705–724 (2008).
15. Bradley, L. D. *et al.* Discovery of a very bright strongly lensed galaxy candidate at  $z \sim 7.6$ . *Astrophys. J.* **678**, 647–654 (2008).
16. Zheng, W. *et al.* Bright strongly lensed galaxies at redshift  $z \sim 6-7$  behind the clusters Abell 1703 and CL0024+16. *Astrophys. J.* **697**, 1907–1917 (2009).
17. Bouwens, R. J. *et al.*  $z \sim 7-10$  galaxies behind lensing clusters: contrast with field search results. *Astrophys. J.* **690**, 1764–1771 (2009).
18. Webster, R. L., Hewett, P. C., Harding, M. E. & Wegner, G. A. Detection of statistical gravitational lensing by foreground mass distributions. *Nature* **336**, 358–359 (1988).
19. Nollenberg, J. G. & Williams, L. L. R. Galaxy-quasar correlations between APM galaxies and Hamburg-ESO QSOs. *Astrophys. J.* **634**, 793–805 (2005).
20. Scranton, R. *et al.* Detection of cosmic magnification with the Sloan Digital Sky Survey. *Astrophys. J.* **633**, 589–602 (2005).
21. Windhorst, R. A., Cohen, S. H., Jansen, R. A., Conselice, C. & Yan, H. How JWST can measure first light, reionization and galaxy assembly. *N. Astron. Rev.* **50**, 113–120 (2006).
22. Schechter, P. An analytic expression for the luminosity function for galaxies. *Astrophys. J.* **203**, 297–306 (1976).
23. Pei, Y. C. Magnification of quasars by cosmologically distributed gravitational lenses. *Astrophys. J.* **440**, 485–500 (1995).
24. Greif, T. H., Johnson, J. L., Bromm, V. & Klessen, R. S. The first supernova explosions: energetics, feedback, and chemical enrichment. *Astrophys. J.* **670**, 1–14 (2007).
25. Hathi, N. P. *et al.* UV-dropout galaxies in the GOODS-South Field from WFC3 early release science observations. *Astrophys. J.* **720**, 1708–1716 (2010).
26. Oguri, M. *et al.* The Sloan Digital Sky Survey quasar lens search. III. Constraints on dark energy from the third data release quasar lens catalog. *Astron. J.* **135**, 512–519 (2008).
27. Choi, Y., Park, C. & Vogeley, M. S. Internal and collective properties of galaxies in the Sloan Digital Sky Survey. *Astrophys. J.* **658**, 884–897 (2007).
28. Huterer, D., Keeton, C. R. & Ma, C. Effects of ellipticity and shear on gravitational lens statistics. *Astrophys. J.* **624**, 34–45 (2005).
29. Komatsu, E. *et al.* Five-year Wilkinson Microwave Anisotropy Probe observations: cosmological interpretation. *Astrophys. J., Suppl.* **180**, 330–376 (2009).
30. Windhorst, R. A. *et al.* High resolution science with high redshift galaxies. *Adv. Space Res.* **41**, 1965–1971 (2008).

**Supplementary Information** is linked to the online version of the paper at [www.nature.com/nature](http://www.nature.com/nature).

**Acknowledgements** We thank K.-H. Chae for discussing results of his lensing calculations. J.S.B.W. was supported in part by a QE-II fellowship and grants from the Australian Research Council. H.Y. acknowledges support from the long-term fellow-ship programme of the Center for Cosmology and AstroParticle Physics (CCAPP) at The Ohio State University. H.Y. and R.A.W. were supported by the Space Telescope Science Institute, which is operated by the Association of Universities for Research in Astronomy, Inc. R.A.W. was supported by a NASA JWST Interdisciplinary Scientist grant.

**Author Contributions** J.S.B.W. performed the calculations of lensing probabilities. H.Y. measured the distributions of galaxy properties from the HUDF. All authors were involved in the conception of the work, discussing the results, and writing the manuscript.

**Author Information** Reprints and permissions information is available at [www.nature.com/reprints](http://www.nature.com/reprints). The authors declare no competing financial interests. Readers are welcome to comment on the online version of this article at [www.nature.com/nature](http://www.nature.com/nature). Correspondence and requests for materials should be addressed to J.S.B.W. ([swyithe@unimelb.edu.au](mailto:swyithe@unimelb.edu.au)).